ANALYSIS OF DIFFRACTIONS IN DIP-ANGLE GATHERS FOR TRANSVERSELY ISOTROPIC MEDIA

YOGESH ARORA and ILYA TSVANKIN

Center for Wave Phenomena, Colorado School of Mines, Golden, CO 80401, U.S.A.
yarora@mymail.mines.edu

(Received May 14, 2018; revised version accepted September 6, 2018)

ABSTRACT

Arora, Y. and Tsvankin, I., 2018. Analysis of diffractions in dip-angle gathers for transversely isotropic media. *Journal of Seismic Exploration*, 27: 515-530.

Diffractions can supplement reflected waves in anisotropic velocity analysis because they increase the aperture and may illuminate parts of the model that do not produce strong reflections. However, enhancement of diffractions and their separation from the more intensive reflections remains a challenging task, especially if the velocity model is not accurate. Here, we analyze diffraction events in dip-angle common-image gathers (CIGs) computed with Kirchhoff migration for transversely isotropic (TI) media. If the velocity model is sufficiently accurate, dip-angle CIGs make it possible to generate diffraction-based depth images using a muting function that depends on reflector dip. We demonstrate application of this methodology to anisotropic diffraction imaging of synthetic data and present a field-data example from the Gulf of Mexico. In the presence of errors in the TI parameters, diffraction and reflection events exhibit different moveout distortions in dip-angle CIGs. In particular, numerical examples show that the moveout of diffractions is sensitive to the key anisotropy parameter η. Therefore, diffractions in the dip-angle domain could be employed in migration velocity analysis (MVA) to refine the anisotropic velocity model.

KEY WORDS: diffracted waves, dip-angle gathers, anisotropy, transverse isotropy, Kirchhoff migration, diffraction imaging.

0965-0651/18/$5.00

INTRODUCTION

Diffractions can be helpful in anisotropic parameter estimation because they carry information from a wide range of propagation angles (e.g., Waheed et al., 2013a,b) and for spatial locations not illuminated by reflections. Diffraction events produced by discontinuities (e.g., faults, fractures, and other geologic features) and certain strong heterogeneities have been employed to refine isotropic velocity models. For example, local slant-stacks (Harlan et al., 1984) and the minimum entropy (ME) norm (De Vries and Berkhout, 1984) were applied to focus diffractions on common-offset sections and perform velocity analysis. Söllner et al. (2002) extend the focusing-based normal-moveout velocity analysis of diffractions to 3D common-offset sections. Fomel et al. (2007) use a velocity continuation method for migration velocity analysis (MVA) of zero-offset diffraction time images. Techniques designed to incorporate reflections and diffractions simultaneously into isotropic velocity analysis include 2D stereotomography (Billette et al., 2003) and wave-equation MVA (Sava et al., 2005).

One of the main challenges in utilizing diffractions for velocity analysis is separating them from reflections, which usually dominate surface seismic data (e.g., Klem-Musatov et al., 1994; Khaidukov et al., 2004). Existing methodologies for diffraction separation are mostly limited to isotropic media and typically require accurate velocity models (Khaidukov et al., 2004; Kozlov et al., 2004; Berkovitch et al., 2009; Moser and Howard, 2008; Sturzu et al., 2013). Arora and Tsvankin (2016) develop a specularity-based method for separating diffractions in anisotropic media and apply it to 2D VTI (TI with vertical symmetry axis) media. Images of diffraction events can supplement reflection-based interpretation in applications such as fracture characterization (Al-Dajani and Fomel, 2010) and time-lapse seismic monitoring (Alonaizi et al., 2014).

Producing well-focused depth images from diffractions typically requires model updating through migration velocity analysis. Audebert et al. (2002) introduce the so-called dip-angle CIGs, in which the distinct moveout signature of diffractions can help separate them from reflection arrivals (Landa et al., 2008). Also, similar to reflections in surface-offset-based gathers, diffraction events exhibit residual moveout in dip-angle gathers when the velocity model is inaccurate. The possibility of performing diffraction-based isotropic velocity analysis of poststack data in the dip-angle domain is explored by Reshef and Landa (2009) and Klokov and Fomel (2012).

Here, dip-angle CIGs are computed from prestack reflection data in TI media using Kirchhoff depth migration. First, we describe a methodology for

constructing dip-angle CIGs and analyze the signatures of both reflections and diffractions in that domain. Then dip-angle gathers are employed to generate diffraction-based depth images for a VTI ramp model, the VTI Marmousi model, and field data from the Gulf of Mexico. Finally, we analyze the sensitivity of diffraction and reflection events in dip-angle CIGs to errors in the interval parameters of layered VTI media and discuss the possibility of refining the anisotropic velocity model by minimizing the residual moveout of diffractions.

CONSTRUCTION OF DIP-ANGLE CIGs AND DIFRACTION-BASED IMAGES

In 2D Kirchhoff migration, the contributions of available seismic traces at any image point ($\mathbf{X}$) can be described by summation over the migration-dip and scattering angles (e.g., Bleistein et al., 2013). The angle between the source-side slowness vector ($\mathbf{P}$) and the receiver-side slowness vector ($\mathbf{P}_r$) is called the scattering angle (ψ) (Fig. 1). The sum of the slowness vectors ($\mathbf{P}_s + \mathbf{P}_r$) represents the migration-dip direction (Audebert et al., 2002; Brandsberg-Dahl et al., 2003), which is aligned with the interface normal for specular reflections migrated with the actual velocity. Hence, the migration-dip angle (ϕ) with the vertical can be computed as

$$\phi = \cos^{-1}\left(\frac{(\mathbf{P_S} + \mathbf{P_r})\cdot\mathbf{z}}{|\mathbf{P_S} + \mathbf{P_r}|}\right), \tag{1}$$

where $\mathbf{z}$ is a vertical unit vector. Imaged data $I(\mathbf{X}, \phi, \psi)$, with the migration-dip (ϕ) and scattering (ψ) angles as the additional dimensions, can be efficiently produced using Kirchhoff migration (e.g., Hale, 1992). The conventional depth image $I(\mathbf{X})$ is obtained by summation over both ϕ and ψ. The dip-angle gathers $I(\mathbf{X}, \phi)$ are computed by summing over just the scattering angles (ψ), with the angle ϕ found from eq. (1).

In dip-angle CIGs created at the scatterer locations with the actual velocity field, reflections are curved, whereas diffractions are flat (Landa et al., 2008; Reshef and Landa, 2009). An appropriate taper function based on the normal vectors $\mathbf{n}$ can be applied to dip-angle gathers to mute the apex of the curved events, which suppresses reflection energy. Then stacking along the dip-angle axis enhances diffractions and yields a diffraction-based image. Here, we apply this methodology to diffraction processing in acoustic VTI media.

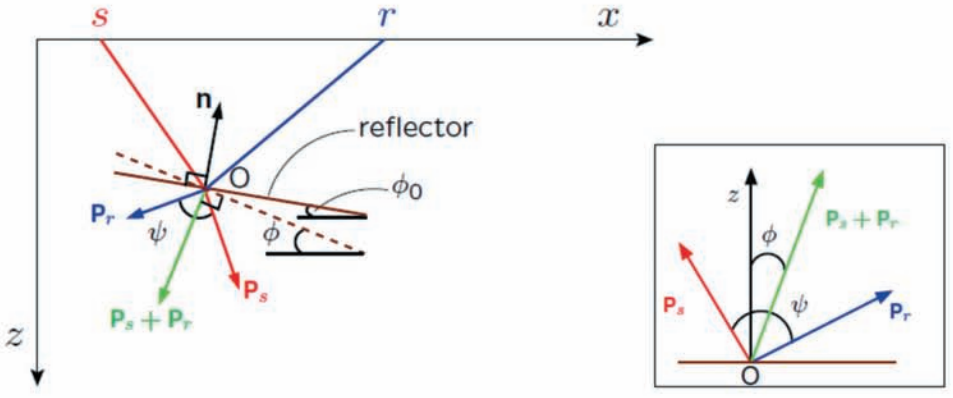

Fig. 1. Image point O on a dipping reflector (dip ϕ_0) for a certain source (s) – receiver (r) pair. $\mathbf{P}_S$ and $\mathbf{P}_r$ denote the source- and receiver side slowness vectors, and **n** is the reflector normal. The migrated dip ϕ corresponds to the direction orthogonal to $\mathbf{P}_S + \mathbf{P}_r$. The inset shows the scattering (ψ) and dip (ϕ) angles.

Numerical examples

First, we compute dip-angle CIGs for the diffraction ramp model in Fig. 2a used by Arora and Tsvankin (2016). Two locations (the vertical blue lines in Fig. 2b) are chosen to analyze the signature of both specular reflections and nonspecular diffractions. The gather located at x = 1.4 km includes two scatterers (termination points of the interface segments) at depths close to z = 2.5 km and 3.0 km (Fig. 3a). These scatterers produce relatively weak diffractions, whose moveouts are flat because the velocity model is accurate. In contrast, the reflector at depth z = 1.0 km generates a strong curved event.

Only reflectors are present below surface location x = 2.2 km, and the corresponding reflection events in the dip-angle gather are curved (Fig. 3b). The additional curved events with steep moveouts are produced by the segments of the truncated reflectors (according to the size of the Fresnel zone) near x = 1.4 km. The quasilinear events in both gathers (at x = 1.4 km and x = 2.2 km) are diffractions from scatterers shifted laterally from the CIG location. The flatness of diffractions in dip-angle CIGs computed with an accurate velocity model allows one to perform diffraction separation. Here, we use an apex removal technique to suppress reflection energy and produce a depth image from diffractions.

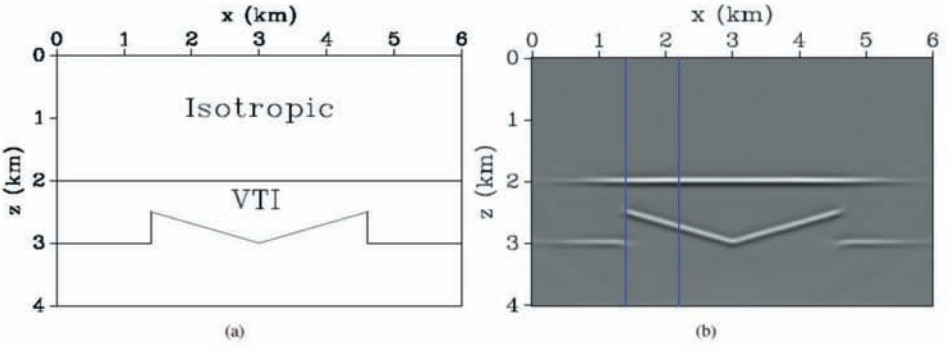

Fig. 2. (a) VTI ramp model where the P-wave velocity in the isotropic overburden is 3.1 km/s, and the relevant Thomsen parameters of the VTI layer are V_{P0} = 3.3 km/s, $\varepsilon = 0.24$, and $\delta = 0.14$. (b) The conventional Kirchhoff depth image with the vertical blue lines marking the locations of the CIGs used below.

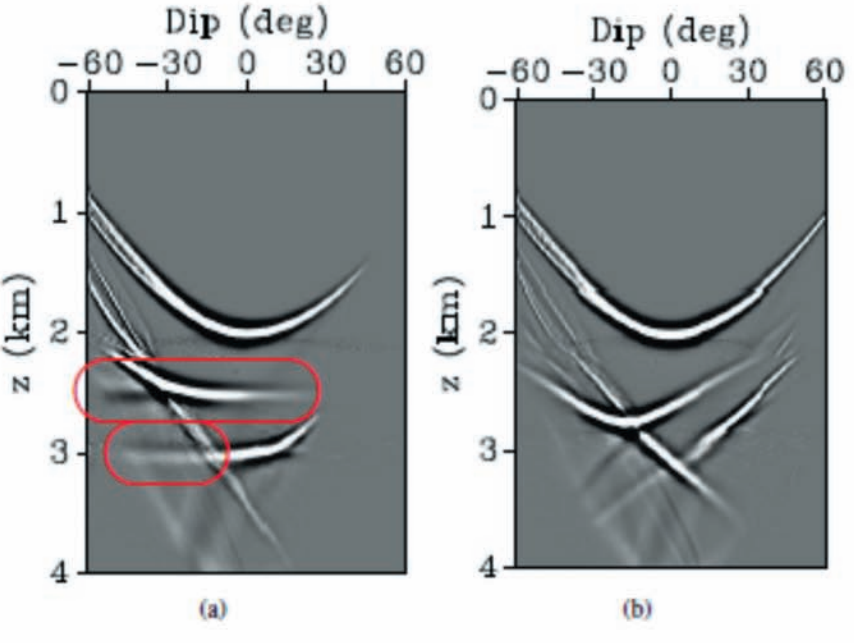

Fig. 3. Dip-angle gathers for the ramp model in Fig. 2a at locations (a) x = 1.4 km, and (b) x = 2.2 km. Encircled are the diffraction events discussed in the text.

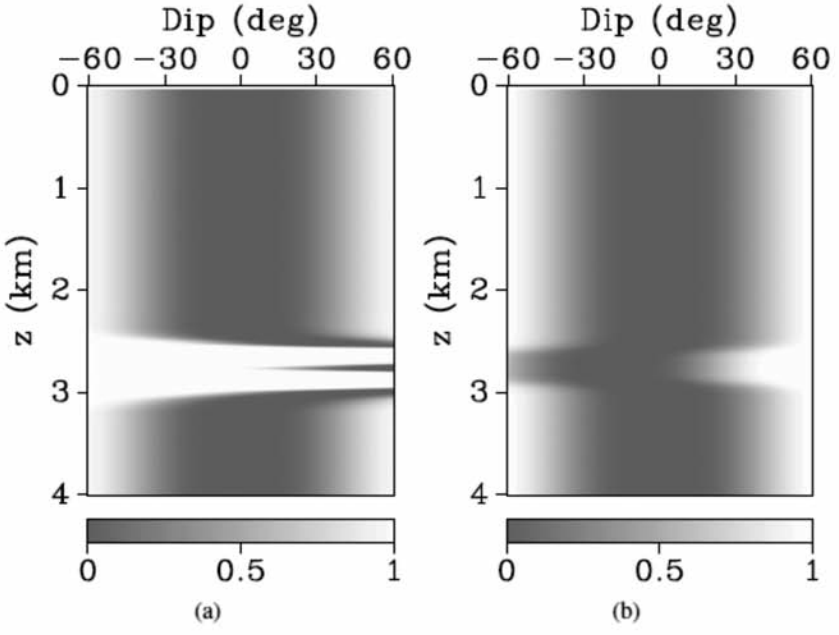

Fig. 4. Mask for the dip-angle gathers in Fig. 3.

The apex (or stationary point) of a curved reflection event in the dip-angle domain (e.g., see Fig. 3) corresponds to the actual interface dip (Bleistein et al., 2013). As suggested by Klokov and Fomel (2012), we construct a mask (Fig. 4) using dip information (vector **n**) to mute the reflections at their apex. Stacking along the dip axis after the reflections have been suppressed (Fig. 5) produces a depth image primarily from diffractions (Fig. 6), which is comparable to that obtained by Arora and Tsvankin (2016) using a specularity-based method. It should be noted that the mask also mutes some of the diffraction energy, especially if diffractions are curved due to velocity errors. Hence, the main shortcoming of this method is its reliance on the accuracy of the velocity model.

Next, we apply this method of constructing diffraction-based images to the VTI version of the structurally complex Marmousi model (Alkhalifah, 1997). Several scatterers, created by the intersections of faults with layer boundaries (Fig. 7), are not clearly visible on the conventional reflection-based depth image (Fig. 8a). Diffraction separation is performed in the dip-angle gathers generated with the actual velocity field. Migrating diffractions obtained from the processed dip-angle gathers substantially enhances scatterers, although the image contains some residual reflection energy (Fig.8b).

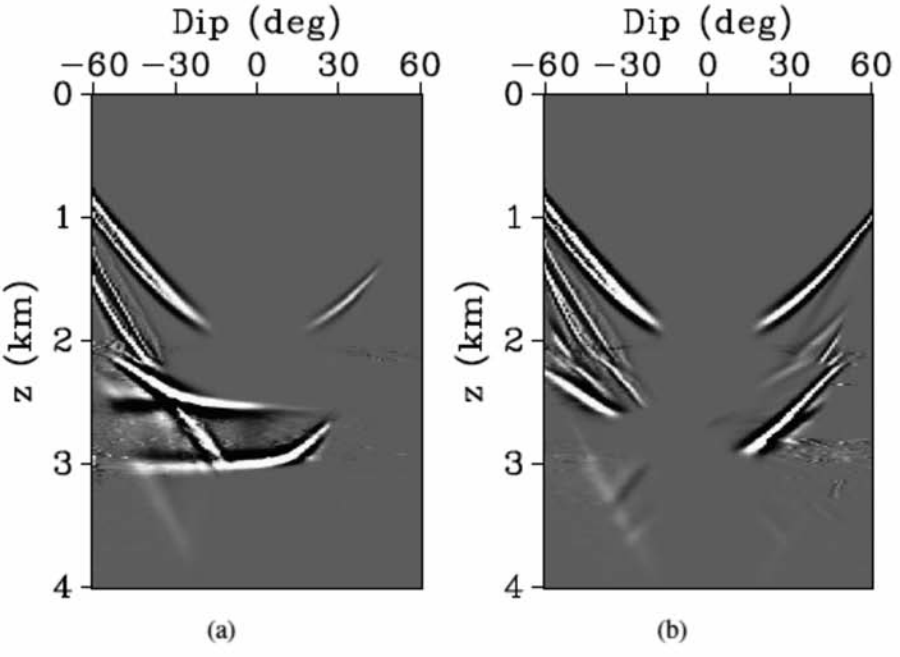

Fig. 5. Dip-angle gathers from Fig. 3 after applying the mask in Fig. 4. Stacking along the dip-angle axis suppresses reflections events.

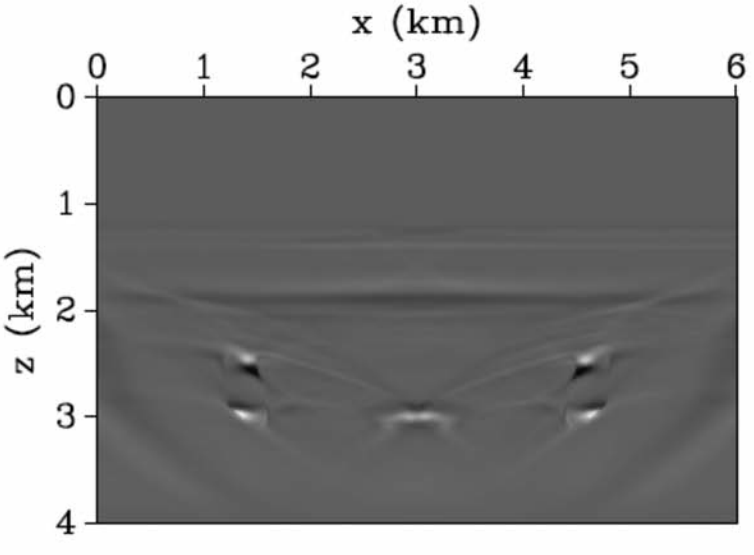

Fig. 6. Depth image from diffractions for the model in Fig. 2a. The reflections in the dip-angle gathers (Fig. 3) are muted using the mask in Fig. 4.

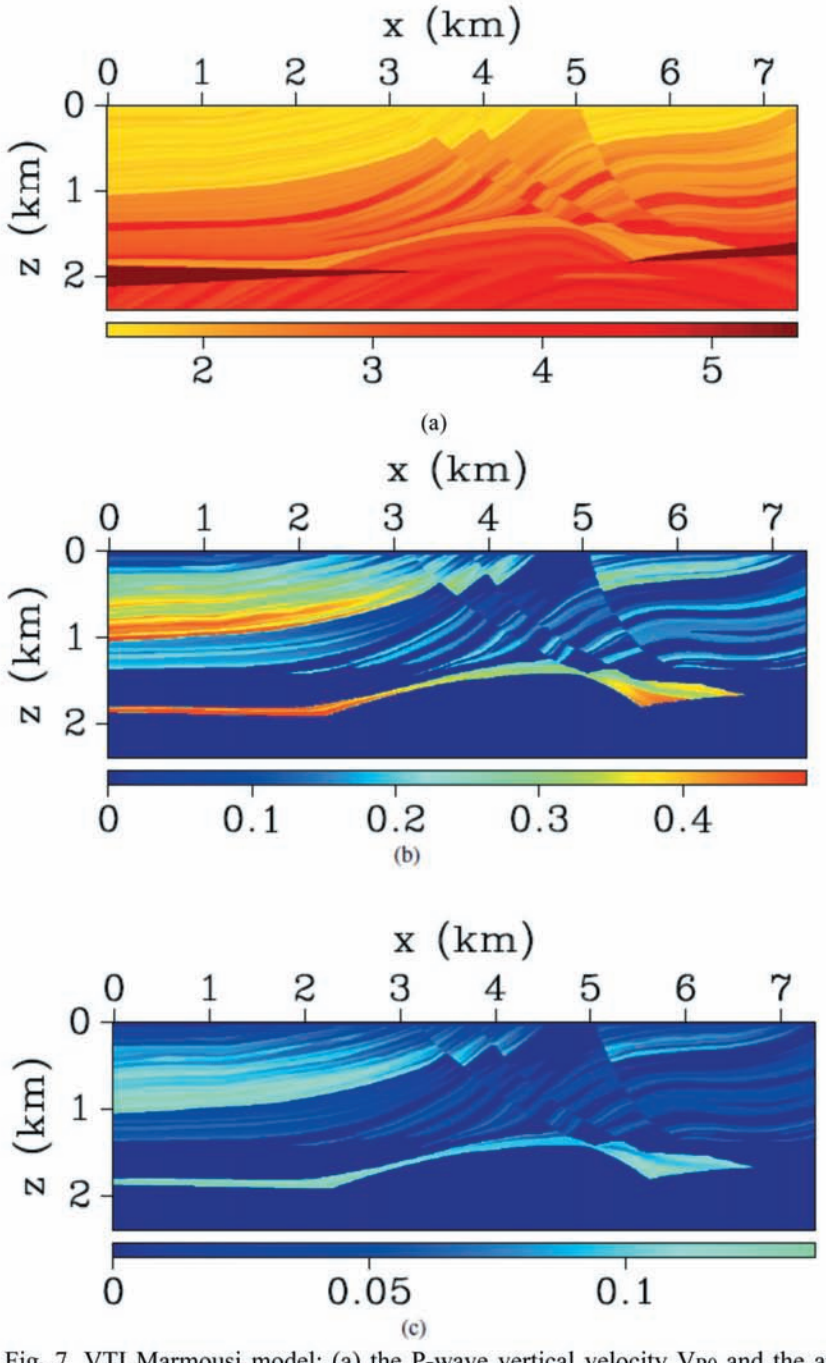

Fig. 7. VTI Marmousi model: (a) the P-wave vertical velocity V_{P0} and the anisotropy coefficients (b) ε, and (c) δ.

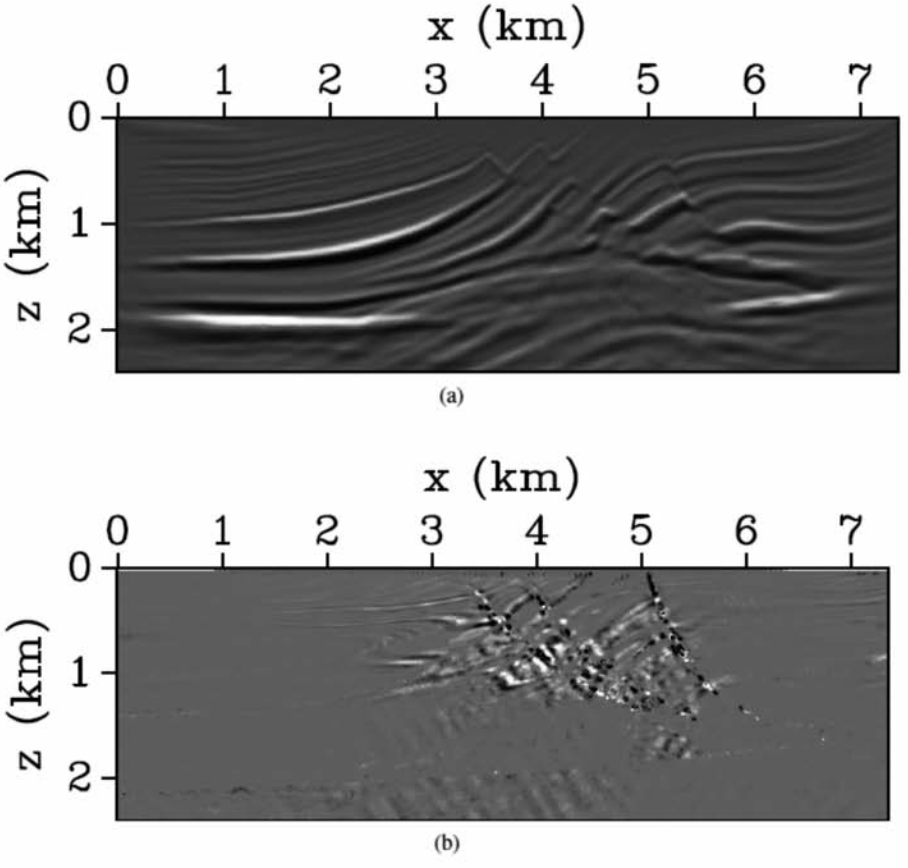

Fig. 8. (a) Conventional (reflection-based), and (b) diffraction-based depth images for the model in Fig. 7. Both images are computed with the actual velocity model.

Field-data example

Finally, the method is tested on a 2D deep-water line from the Mississippi Canyon in the Gulf of Mexico (Verschuur and Prein, 1999). The data were acquired in streamer geometry with 1000 shot gathers that include 180 receivers each. Small-scale faults and rough edges of the salt body produce diffractions visible in common-offset sections (Fig. 9). We use the isotropic P-wave velocity model provided with the data (Fig. 10a) to compute a migrated image (Fig. 10b) and dip-angle CIGs (Fig. 11). Prior to depth imaging, reflections are filtered out in dip-angle gathers using normal vectors obtained by applying plane-wave destructor filters (Fomel, 2002).

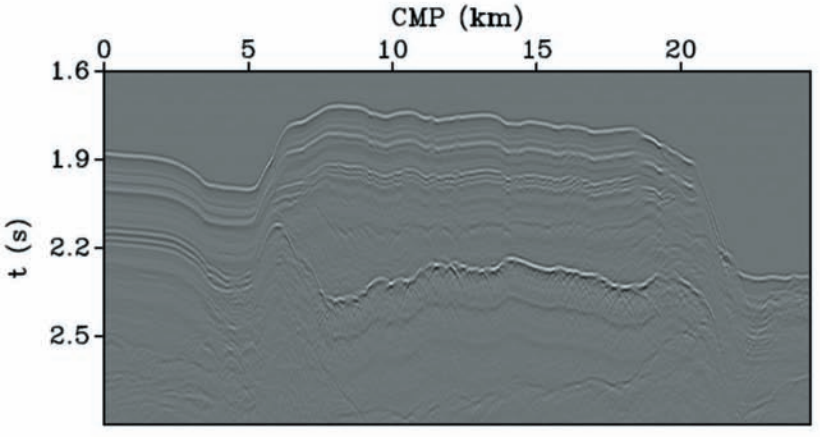

Fig. 9. Common-offset section for a line from the Gulf of Mexico.

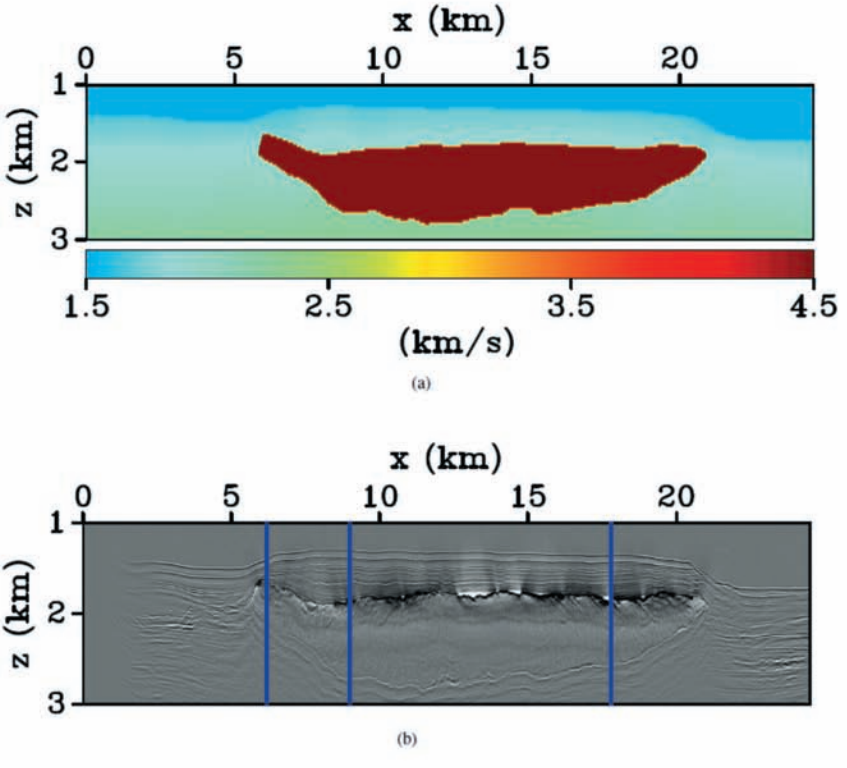

Fig. 10. (a) Isotropic P-wave velocity field and (b) the corresponding depth image. The vertical blue lines mark the locations of the CIGs used below.

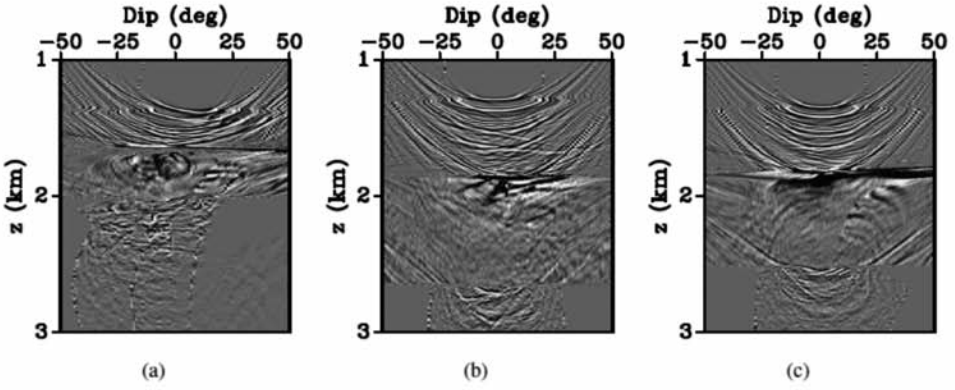

Fig. 11. Dip-angle gathers of the field data (Figs. 9 and 10) at locations (a) x = 2.32 km, (b) x = 3.37 km and (c) x = 6.67 km.

The rough edges around the salt body are substantially enhanced in the resulting diffraction-based depth image (Fig. 12). Also, the salt flanks, which often reside in shadow zones for reflections, are better illuminated by the cluster of scatterers. However, small-scale faults at the top of the salt are not well focused, likely due to the inaccuracy of the velocity model. This example shows that diffraction imaging could help delineate salt boundaries. Still, it should be noted that diffractions can only supplement reflection-based images in subsalt exploration.

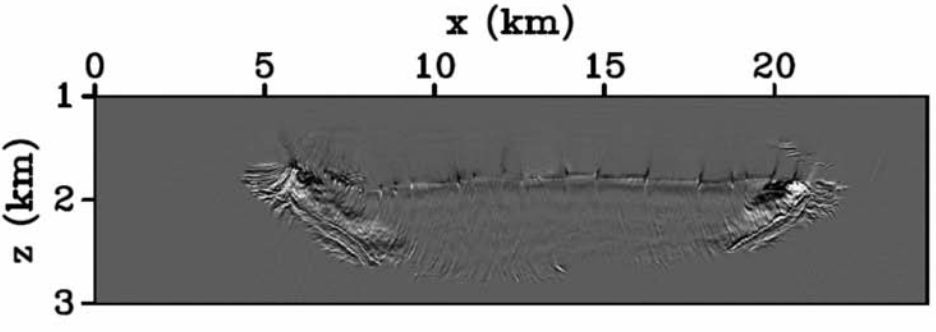

Fig. 12. Diffraction-based depth image of the field data.

INFLUENCE OF VTI PARAMETERS ON DIP-ANGLE GATHERS

The potential of dip-angle CIGs for separating diffractions and employing them in isotropic MVA was shown by Landa et al. (2008), Reshef

and Landa (2009), and Klokov and Fomel (2012). A key step in implementing model updating (MVA) using diffractions is their separation from reflections when the velocity field is still inaccurate. Here, we discuss the possibility of using diffractions in building TI velocity models.

Properties of dip-angle CIG's

To analyze dip-angle gathers in the presence of anisotropy, we consider the VTI model in Fig. 13, which includes a point scatterer along with horizontal and dipping reflectors. Our goal is to assess the influence of errors in the P-wave zero-dip NMO velocity V_{nmo}, the anellipticity parameter η, and Thomsen parameter δ on the reflection and diffraction events in the dip-angle domain. As discussed by Alkhalifah and Tsvankin (1995) and Tsvankin (2012), the parameters V_{nmo} and η are primarily responsible for focusing reflections in time and depth migration for VTI media, while δ controls migrated reflector depths.

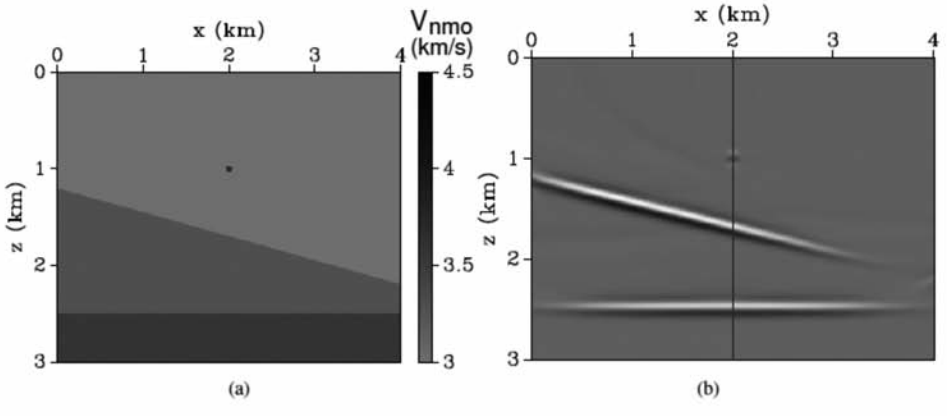

Fig. 13. (a) VTI model with V_{nmo} = 3.28 km/s in the overburden and 3.61 km/s in the layer below the dipping interface. The anisotropy parameters η = 0.22 and δ = 0.10 are the same in both layers. (b) A conventional depth image with the vertical blue line marking the CIG used below.

Errors in V_{nmo} and η for the model in Fig. 13 cause a noticeable residual moveout for the diffraction from the scatterer at z = 1 km (i.e., the diffraction event is no longer flat). The parameters V_{nmo} and η influence the moveout of reflection events as well but reflections are curved even for the actual model (Figs. 14 and 15). Note that inaccurate values of V_{nmo} produce residual moveout for diffractions at almost all dip angles, while the residuals due to errors in η become pronounced only at relatively large dips. Such a behavior is expected because the influence of η on the NMO velocity of dipping events increases with dip (Tsvankin, 2012). Errors in the parameter δ

distort the imaged depths of the scatterer and reflectors but the diffraction events remain flat (Fig. 16). In contrast to diffractions, the shape of the reflection events in dip-angle gathers is not sufficiently sensitive to the VTI parameters.

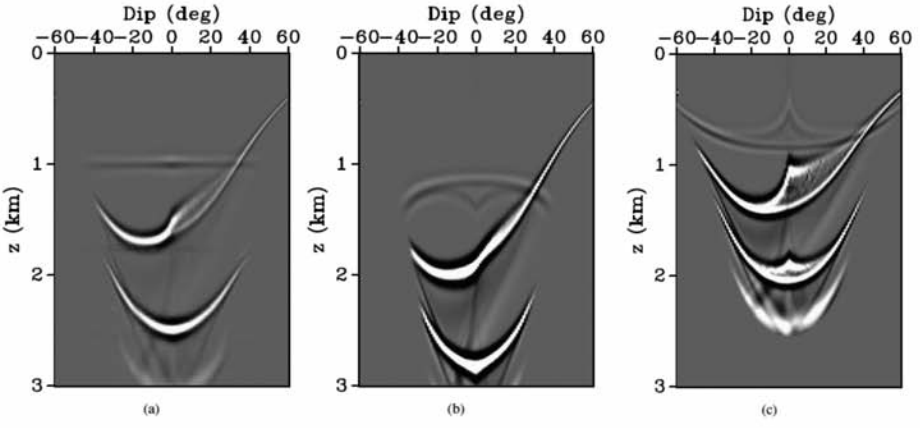

Fig. 14. Dip-angle CIGs for the model in Fig. 13 (x = 2.0 km) computed with the (a) actual velocity field; (b) overstated V_{nmo} = 3.77 km/s (constant throughout the model); and (c) understated constant V_{nmo} = 2.79 km/s.

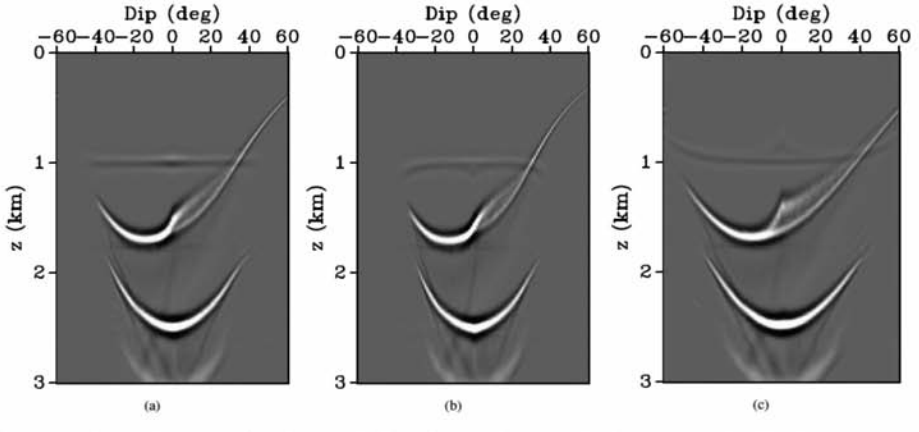

Fig. 15. Dip-angle CIGs for the model in Fig. 13 (x = 2.0 km) computed with the (a) actual velocity field; (b) overstated η = 0.37 (constant throughout the model); and (c) understated constant η = 0.07.

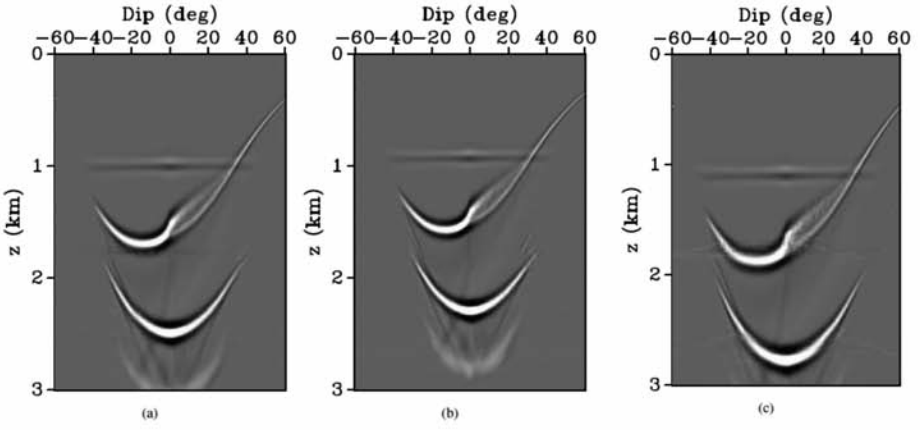

Fig. 16. Dip-angle CIGs for the model in Fig. 13 (x = 2.0 km) computed with the (a) actual velocity field; (b) overstated $\delta = 0.20$ (constant throughout the model); and (c) understated constant $\delta = 0$.

DISCUSSION: **Migration Velocity Analysis (MVA) using difractions**

Reshef and Landa (2009) and Klokov and Fomel (2012) use velocity-scanning methods to perform isotropic MVA of diffraction events in dip-angle gathers. This approach may not be practical for anisotropic parameter estimation because it does not account for realistic lateral heterogeneity and is computationally expensive for field data. Also, it is necessary to obtain the locations of the scatterers from the diffraction-based depth images. Knowledge of those locations is needed to construct dip-angle CIGs, which provide the input for tomographic model updating.

Instead of velocity scanning, the residual moveout of diffractions in dip-angle gathers could be directly employed to refine the anisotropic velocity field. The residual moveout of reflected waves in surface-offset CIGs has been widely used in MVA and reflection tomography to build isotropic and TI velocity models (e.g., Liu, 1997; Sarkar and Tsvankin, 2004; Woodward et al., 2008; Wang and Tsvankin, 2013). Efficient separation of diffractions that preserves their residual moveout in dip-angle CIGs is a necessary condition for diffraction-based velocity analysis. Therefore, the initial model (presumably obtained from reflections) should be sufficiently accurate to suppress reflections without significantly damaging diffraction events. Velocity updates obtained through the diffraction-based anisotropic MVA should improve the focusing of scatterers and, potentially, the quality of reflection-based images as well. Implementation of this approach is the subject of ongoing work.

CONCLUSIONS

We discussed diffraction-based imaging in TI media using dip-angle common-image gathers. These gathers can be generated by Kirchhoff depth migration with subsequent summation over the scattering angles. If migration is performed with an accurate velocity field, diffractions in dip-angle CIGs are flat, whereas reflections are curved. Hence, reflection events can be muted using a mask computed from the interface normal vectors.

We successfully applied this technique to synthetic models (including VTI Marmousi) and field data from the Gulf of Mexico to produce diffraction-based depth images from dip-angle gathers. However, separation of diffractions based on the shape of their moveout may become ineffective if the velocity model is not sufficiently accurate.

We also perturbed the VTI parameters V_{nmo}, η, and δ to analyze the sensitivity of diffractions and reflections in the dip-angle domain to distortions of the velocity field. The residual moveout developed by diffractions for inaccurate values of V_{nmo} and η potentially could be used in a tomographic algorithm to update these parameters. Errors in the NMO velocity cause the residual moveout for almost all dips, whereas the influence of η becomes substantial for relatively steep events. For the model used here, changes in the parameter δ only shift imaged events in depth. However, a strong lateral variation of δ above a scatterer could produce residual moveout for the corresponding diffraction event (Li et al., 2016). In contrast, the moveout of reflections in dip-angle gathers does not readily provide suitable criteria for model updating.

REFERENCES

Al-Dajani, A. and Fomel, S., 2010. Fractures detection using multi-azimuth diffractions focusing measure: Is it feasible? Expanded Abstr., 80th Ann. Internat. SEG Mtg., Denver: 287-291.

Alkhalifah, T., 1997. An anisotropic Marmousi model: SEP-95. Stanford Explor. Proj.: 265-282.

Alkhalifah, T. and Tsvankin, I., 1995. Velocity analysis for transversely isotropic media. Geophysics, 60: 1550-1566.

Alonaizi, F., Pevzner, R., Bona, A., Alshamry, M., Caspari, E. and Gurevich, B., 2014. Application of diffracted wave analysis to time-lapse seismic data for CO_2 leakage detection. Geophys. Prosp., 60: 197-209.

Arora, Y. and Tsvankin, I., 2016. Separation of diffracted waves in transversely isotropic media. Studia Geophys. Geodaet., 60: 487-499.

Audebert, F., Froidevaux, P., Rakotoarisoa, H. and Lucas, J.S., 2002. Insights into migration in the angle domain. Expanded Abstr., 72nd Ann. Internat. SEG Mtg., Salt Lake City: 1188-1191.

Berkovitch, A., Belfer, I., Hassin, Y. and Landa, E., 2009. Diffraction imaging by multifocusing. Geophysics, 74(6): WCA75-WCA81.

Billette, F., Bégat, S.L., Podvin, P. and Lambaré, G., 2003. Practical aspects and applications of 2D stereotomography. Geophysics, 68: 1008-1021.

Bleistein, N., Cohen, J.K. and Stockwell Jr., J.W., 2013. Mathematics of Multi-dimensional Seismic Imaging, Migration, and Inversion. Springer Science & Business Media, 13, New York.

Brandsberg-Dahl, S., Ursin, B. and de Hoop, M., 2003. Seismic velocity analysis in the scattering- angle/azimuth domain. Geophys. Prosp., 51: 295-314.
De Vries, D. and Berkhout, A.J., 1984. Velocity analysis based on minimum entropy. Geophysics, 49: 2132-2142.
Fomel, S., 2002. Applications of plane-wave destruction filters. Geophysics, 67:1946-1960.
Fomel, S., Landa, E. and Taner, M., 2007. Poststack velocity analysis by separation and imaging of seismic diffractions. Geophysics, 56(6): U89-U94.
Hale, D., 1992. Migration by the Kirchhoff, slant stack, and Gaussian beam methods. CWP Project Review Report.
Harlan, W.S., Claerbout, J.F. and Rocca, F., 1984. Signal/noise separation and velocity estimation. Geophysics, 49: 1869-1880.
Khaidukov, V., Landa, E. and Moser, T.J., 2004. Diffraction imaging by focusing-defocusing: An outlook on seismic superresolution. Geophysics, 69: 1478-1490.
Klem-Musatov, K.D., Hron, F., Lines, L.R. and Meeder, C.A., 1994. Theory of Seismic Diffractions. SEG, Tulsa, OK.
Klokov, A. and Fomel, S., 2012. Separation and imaging of seismic diffractions using migrated dip-angle gathers. Geophysics, 77(6): S131-S143.
Kozlov, E., Barasky, N., Korolev, E., Antonenko, A. and Koshchuk, E., 2004. Imaging scattering objects masked by specular reflections. Expanded Abstr., 74th Ann. Internat. SEG Mtg., Denver: 1131-1134.
Landa, E., Fomel, S. and Reshef, M., 2008. Separation, imaging, and velocity analysis of seismic diffractions using migrated dip-angle gathers. Expanded Abstr., 78th Ann. Internat. SEG Mtg., Las Vegas.
Li, V., Tsvankin, I. and Alkhalifah, T., 2016. Analysis of RTM extended images for VTI media. Geophysics, 81(3): S139-S150.
Liu, Z., 1997. An analytical approach to migration velocity analysis. Geophysics, 62: 1238-1249.
Moser, T. and Howard, C., 2008. Diffraction imaging in depth. Geophys. Prosp., 56: 627-641.
Reshef, M. and Landa, E., 2009. Post-stack velocity analysis in the dip-angle domain using diffractions. Geophys. Prosp., 57: 811-821.
Sarkar, D. and Tsvankin, I., 2004. Migration velocity analysis in factorized VTI media. Geophysics, 69: 708-718.
Sava, P.C., Biondi, B. and Etgen, J., 2005. Wave-equation migration velocity analysis by focusing diffractions and reflections. Geophysics, 70: U19-U27.
Söllner, W. and Yang, W., 2002. Diffraction response simulation: a 3D velocity inversion tool. Expanded Abstr., 72nd Ann. Internat. SEG Mtg., Salt Lake City: 2293-2296.
Sturzu, I., Popovici, A.M., Tanushev, N., Musat, I., Pelissier, A. and Moser, T.J., 2013. Specularity gathers for diffraction imaging. Extended Abstr., 75th EAGE Conf., London.
Tsvankin, I., 2012. Seismic Signatures and Analysis of Reflection Data in Anisotropic Media, 3rd ed. SEG, Tulsa, OK.
Verschuur, D. and Prein, R., 1999. Multiple removal results from Delft University. The Leading Edge, 18: 86-91.
Waheed, U.B., Alkhalifah, T. and Stovas, A., 2013a. Diffraction traveltime approximation for TI media with an inhomogeneous background. Geophysics, 78(5): WC103-WC111.
Waheed, U.B., Stovas, A. and Alkhalifah, T., 2013b. Anisotropic parameter inversion in VTI media using diffraction data. Expanded Abstr., 83rd Ann. Internat. SEG Mtg., Houston.
Wang, X. and Tsvankin, I., 2013. Multiparameter TTI tomography of P-wave reflection and VSP data. Geophysics, 78(5): WC51-WC63.
Woodward, M.J., Nichols, D., Zdraveva, O., Whitfield, P. and Johns, T., 2008. A decade of tomography. Geophysics, 73(5): VE5-VE11.